Mechanism of the Dihydroorotase Reaction†

Tamiko N. Porter, Yingchun Li, and Frank M. Raushel*

Department of Chemistry, P.O. Box 30012, Texas A&M University, College Station, Texas 77842-3012

Received August 6, 2004; Revised Manuscript Received October 13, 2004

ABSTRACT: Dihydroorotase (DHO) is a zinc metalloenzyme that functions in the pathway for the biosynthesis of pyrimidine nucleotides by catalyzing the reversible interconversion of carbamoyl aspartate and dihydroorotate. A chemical mechanism was proposed on the basis of an analysis of the effects of pH, metal substitution, solvent isotope effects, mutant proteins, and alternative substrates on the enzyme-catalyzed reaction. The pH−rate profiles for the hydrolysis of dihydroorotate or thiodihydroorotate demonstrated that a single group from the enzyme must be unprotonated for maximal catalytic activity. Conversely, the pH−rate profiles for the condensation of carbamoyl aspartate to dihydroorotate showed that a single group from the enzyme must be protonated for maximal catalytic activity. The native zinc ions within the active site of DHO were substituted with cobalt or cadmium by reconstitution of the apoenzyme with divalent cations in the presence of bicarbonate. The ionizations observed in the pH−rate profiles were dependent on the specific metal ion bound to the active site. Mutation of the residue (Asp-250) that hydrogen bonds to the bridging hydroxide (or water) resulted in the loss of catalytic activity. These results are consistent with the formation of a hydroxide bridge between the two divalent cations that functions as the nucleophile during the hydrolysis of dihydroorotate. In addition, Asp-250 is postulated to shuttle the proton from the bridging hydroxide to the leaving group amide during hydrolysis of dihydroorotate. The X-ray crystal structure of DHO showed that the exocyclic α-carboxylate of dihydroorotate is bound to the protein via electrostatic interactions with Arg-20, Asn-44, and His-254. Mutation of these residues resulted in the loss of catalytic activity, indicating that these residues are critical for substrate recognition. The thio analogue of dihydroorotate was found to be a good substrate of the enzyme. A comprehensive chemical mechanism for DHO was proposed on the basis of the experimental findings in this study and the X-ray crystal structure.

Dihydroorotase (DHO)[1] functions in the biosynthesis of pyrimidine nucleotides by catalyzing the reversible cyclization of *N*-carbamoyl L-aspartate to L-dihydroorotate as shown in Scheme 1. An analysis of the amino acid sequences of DHO from multiple species reveals that there are two general classes of this enzyme (*1*). Members of class I are found in higher organisms and are larger than their class II counterparts that are found in many bacteria and fungi. Examples of the class I form of DHO are exemplified by CAD, a multifunctional enzyme found in mammals, insects, and molds. The CAD protein consists of the first three enzymes of the pyrimidine biosynthetic pathway: carbamoyl phosphate synthetase (CPS), aspartate transcarbamoylase (ATC), and DHO (*2*, *3*). Monofunctional examples of class I DHOs are found in Gram-positive bacterial strains, including *Bacillus subtilis*, *Lactobacillus plantarum*, *Enterococcus faecalis*, *Clostridium acetobutylicum*, and *Streptococcus aureus*. The class II enzymes are all monofunctional proteins from Gram-negative bacteria and yeast. Class I proteins have typical subunit molecular masses of ∼45 kDa compared to ∼38 kDa for the class II proteins. Within each class of enzymes, the level of amino acid sequence identity is quite high (>40%), but a low level of sequence identity (<20%) is observed in a comparison of proteins between these two classes. For example, the level of sequence identity between the human (class I) and *Escherichia coli* (class II) forms of DHO is only 17%. There are approximately 17 residues that are fully conserved within the DHO enzymes sequenced to date in both classes of enzyme.

Scheme 1

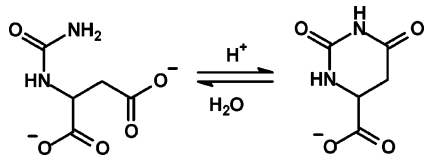

The DHO from hamster was initially reported to contain a single zinc ion that could be replaced with Co^{2+}, Mn^{2+}, or Cd^{2+} with retention of catalytic activity (*4*). However, the X-ray crystal structure of the *E. coli* enzyme demonstrated that the bacterial DHO contains two zinc ions per active site (*5*). The high-resolution structure also confirmed the assignment of DHO as a member of the amidohydrolase superfamily with a $(\beta\alpha)_8$-barrel protein fold and whose binuclear metal center is identical to that previously observed for phosphotriesterase and urease (*5*, *6*). The members of the amidohydrolase superfamily of metalloenzymes function

† This work was supported in part by the National Institutes of Health (GM 33894) and the Robert A. Welch Foundation (A-840).

* To whom correspondence should be addressed. Telephone: (979) 845-3373. Fax: (979) 845-9452. E-mail: raushel@tamu.edu.

[1] Abbreviations: DHO, dihydroorotase; CPS, carbamoyl phosphate synthetase; ATC, aspartate transcarbamoylase; TDO, thiodihydroorotate; QM, C63S/C65S/C121S/C179S quadruple mutation of native DHO.

10.1021/bi048308g CCC: $27.50
Published on Web 11/26/2004

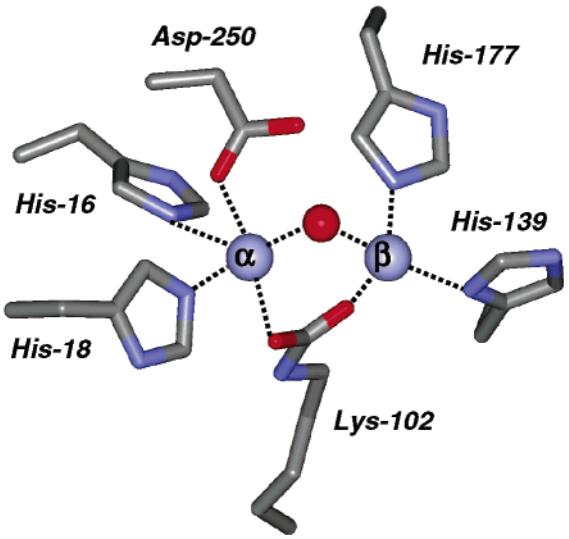

FIGURE 1: Representation of the binuclear metal center within the active site of DHO. The structure was obtained by Thoden et al. (*5*), and the coordinates were obtained from the Protein Data Bank (entry 1J79).

primarily, but not exclusively, as catalysts for hydrolytic reactions at carbon and phosphorus centers. A representation of the binuclear metal center in DHO is presented in Figure 1. The six conserved residues found at the C-terminus of the central β-strands are His-16, His-18, Lys-102, His-139, His-177, and Asp-250. The two zinc ions are bridged by a carbamate functional group formed from the post-translational carboxylation of Lys-102 with CO_2 and a molecule from solvent that is most likely hydroxide.

The reversible reaction catalyzed by DHO is pH-dependent, and the equilibrium constant of the overall reaction as written in Scheme 1 is 1.5×10^6 M^{-1} (*7*). At pH 6.2, the equilibrium between carbamoyl aspartate and dihydroorotate is unity. At lower pH values, the formation of dihydroorotate is favored. Conversely, at higher pH values, the formation of carbamoyl aspartate is dominant. DHO was first crystallized at a pH at which the equilibrium constant for the interconversion between the substrate and product was equal to approximately 1 (*5*). This fortuitous event enabled the structural elucidation of the specific molecular interactions between the substrate or product and the metal center in individual subunits to be unveiled within the same dimer of DHO in the crystalline state. In one subunit of the dimer, dihydroorotate was bound to the active site, while in the adjacent subunit, carbamoyl aspartate was bound. Carbamoyl aspartate coordinates to the binuclear metal center via a bridging interaction through the side chain carboxylate of the substrate. In contrast, the amide carbonyl group of dihydroorotate interacts with the binuclear metal center by direct coordination to the β-metal ion. The bridging hydroxide is more closely associated with the α-metal ion. Electrostatic interactions with the backbone atoms of Leu-222, Ala-266, and Gly-267 stabilize the binding of the substrate and product in the active site of DHO. The most specific contacts between the protein and substrate originate from the side chains of Arg-20, Asn-44, and His-254 via the formation of electrostatic interactions with the free α-carboxylate group of dihydroorotate and carbamoyl aspartate.

In this paper, we provide direct biochemical support for the chemical mechanism first suggested by the molecular contacts observed in the X-ray crystal structure of DHO. The role of Asp-250 in proton transfer reactions is assessed via mutation of the side chain carboxylate of this residue to functional groups that are unable to serve this function. Mutagenesis of specific residues was implemented to probe the functional requirement for the electrostatic interactions of the side chains of Arg-20, Asn-44, and His-254 with the α-carboxylate of dihydroorotate and carbamoyl aspartate. Metal-substituted variants of DHO were prepared to elucidate the roles of the metals in catalysis and to identify the role the bridging hydroxide plays in catalysis. The sulfur analogue of dihydroorotate was analyzed as a substrate for DHO and used to probe the interactions between the amide bond that is formed and broken with the binuclear metal center of DHO.

MATERIALS AND METHODS

Materials. N-Carbamoyl aspartate was purchased from Research Organics. Deuterium oxide was obtained from Cambridge Isotope Laboratories. Platinum pfx DNA polymerase was acquired from Invitrogen, while the remainder of the molecular biology products were from Promega or Stratagene. The buffers, substrates, and other chemicals were acquired from Sigma-Aldrich. The Gene Technology Laboratory of Texas A&M University performed the DNA sequencing reactions and oligonucleotide synthesis. Thiodihydroorotate (TDO) was synthesized using the protocol described by Christopherson et al. (*8*). The structure was confirmed by a comparison of the published proton NMR spectrum and the mass spectrum (ESI, negative ion mode *m*/*z* 173.06, expected *m*/*z* 173.18).

Site-Directed Mutagenesis. The DHO used as the wild-type enzyme in these experiments was altered from the native *pyr*C gene isolated from *E. coli*. Four cysteine residues that are thought to cause sensitivity to oxidation were substituted for serine residues with no loss of activity or change in any other enzymatic property (*9*, *10*). These residues are Cys-63, Cys-65, Cys-121, and Cys-179. The single-point mutations at any one of these sites did not consistently produce a protein that was stable with maximum catalytic activity for an extended period of time. The quadruple mutant (C63S/C65S/C121S/C179S) was stable and had kinetic parameters consistent with previously reported values (*9*, *11*). The DNA template for the remainder of the mutagenesis experiments described in this paper utilized the altered sequence with the mutation of four cysteine residues to serine and designated as the QM protein.

The mutagenesis protocol was PCR-based and involved the use of four primers that produced two overlapping fragments (*12*). The cloning vector in all cases was pBS^+ from Stratagene. A typical reaction mixture contained 2 ng of template DNA, each primer at 4 μM, 1× pfx buffer, 2.0 mM dNTP mix, and 5 units of platinum pfx DNA polymerase. The PCR protocol was used as follows: 2 min at 95 °C, 25 cycles of 1 min at 95 °C, 1 min at 50 °C, and 4 min at 68 °C, followed by 1 cycle of 10 min at 68 °C. The PCR products were digested with *Eco*RI and *Hin*dIII for 2 h at 37 °C, purified, and then ligated with similarly digested pBS^+. XL1 Blue cells were transformed with the ligation

reactions. Cells containing the plasmid were selected on LB plates containing ampicillin. Individual colonies were used to inoculate 5 mL LB cultures, which were grown overnight at 37 °C. The plasmids were isolated from the overnight cultures using the Wizard Mini-Prep SV kit (Promega). The desired mutations were confirmed by sequencing of the isolated DNA.

Protein Purification. The wild-type and mutant forms of DHO were all purified in the same manner. *E. coli* strain X7014a, which lacks a functional gene for dihydroorotase, was obtained from the Yale *E. coli* Genetic Stock Center (Yale University, New Haven, CT) and transformed with the pBS^+ plasmids containing the gene for DHO. For each preparation, large cultures were incubated at 37 °C until they reached mid-log phase, at which point IPTG was added to a concentration of 1.0 mM. After overnight incubation, the cells were collected by centrifugation and resuspended in 50 mM Tris-phosphate (pH 7.0), 100 μM $ZnCl_2$, and 5.0 mM carbamoyl aspartate. The cells were lysed by sonication and the nucleic acids precipitated by the addition of a 2.0% proteamine sulfate solution. After centrifugation, the cell extract was saturated to 60% in ammonium sulfate. After centrifugation, the pellet was resuspended in a minimal amount of buffer and then chromatographed with the aid of an AKTA purifier (Pharmacia) using a Superdex-200 26/60 column. The buffer used for the gel filtration column was 50 mM bis-tris propane (pH 7.0) containing 5.0 mM carbamoyl aspartate. The flow rate was 1.0 mL/min with 1.5 mL fractions being collected. The fractions containing DHO activity were pooled and loaded onto a Resource-Q anion exchange column with the AKTA system. Buffer A was 20 mM bis-tris propane (pH 7.0), while buffer B was the same buffer with 1.0 M NaCl. The protein was eluted from the column by the use of a salt gradient (from 0 to 30% buffer B in 30 column volumes). The flow rate was 4.0 mL/min with 1.0 mL fractions being collected. Fractions were assayed for activity, and those containing DHO were pooled. The purified enzyme was typically stored at −80 °C in 20 mM bis-tris propane (pH 7.0) with 20% glycerol, 100 μM $ZnCl_2$, and 5.0 mM carbamoyl aspartate.

Preparation and Reconstitution of the Apoenzyme. Chelex 100 (Bio-Rad) was used to remove contaminating metals from buffers. The buffers were degassed with argon prior to the addition of enzyme. The apoenzyme was prepared by incubating DHO at a concentration of 1.5 mg/mL for 24 h with 25 mM dipicolinate in 50 mM sodium acetate (pH 5.5) containing 50 mM sodium sulfate, 2.0 mM sodium hydrosulfite, and 30% glycerol. The dipicolinate was removed by dialysis using three changes, 24 h each, of 20 mM sodium acetate (pH 5.8) containing 2.0 mM sodium hydrosulfite and 20% glycerol. To reconstitute the apoenzyme, the protein solution was made 100 mM in Hepes (pH 8.0), 2.0 mM sodium hydrosulfite, and 100 mM potassium bicarbonate. Typical protein concentrations were 0.5−1.0 mg/mL. Excess divalent metal chloride salts at concentrations of 26−130 μM were added to the apoenzyme for reconstitution of catalytic activity. The maximum recovery of activity required incubation for 3 days at 4 °C. Atomic absorption (AA) spectroscopy was used to measure the concentration of each cation in the protein samples. Prior to the performance of AA analysis, the protein solution was passed through a PD10 column (Pharamacia) equilibrated with metal-free buffer to remove excess metal ions. The zinc content per subunit of the purified mutant enzymes was found to be 1.2, 1.2, 0.6, 2.0, and 3.3 for the D250E, D250H, D250N, R20K, and R20Q mutants, respectively.

Enzyme Assays. DHO activity was determined by a direct spectrophotometric assay at 230 nm (*13*). The assays were performed in a 96-well plate using a SPECTRAmax-340 (Molecular Devices) plate reader. Dihydroorotate absorbs at 230 nm with an extinction coefficient of 1.17 mM^{-1} cm^{-1} (*14*). TDO absorbs at 280 nm with an extinction coefficient of 17 mM^{-1} cm^{-1}. The assay volume was 250 μL which corresponds to a path length of 0.69 cm. The buffers for the pH−rate profiles were the potassium salts of MES from pH 5 to 6.75, HEPES from pH 6.75 to 8.5, and TABS from pH 8.5 to 9.5. The buffer concentration in each assay was 50 mM, and the pH was varied in 0.25 unit increments. The pH was measured at the completion of the enzymatic reaction. For the variation of carbamoyl aspartate, the concentration range was 0.05−20 mM. A range of 0.025−1.75 mM was used for the variation of dihydroorotate and TDO. For measurement of the solvent isotope effects, the same reaction conditions were used except that the buffers were prepared in D_2O. Enzyme dilutions were performed in 20 mM Hepes (pH 7.0) prepared with D_2O. The pD of each reaction mixture was measured after completion of the assay by adding 0.4 to the pH electrode reading (*15*). The solvent deuterium isotope effects were determined over the pH range of 5.5−7.0 for the synthesis reaction and over the pH range of 8.0−9.8 for the hydrolysis reaction.

Data Analysis. The kinetic parameters, k_{cat} and k_{cat}/K_m, from the initial velocity experiments were determined from a fit of the data to eq 1, where v is the initial velocity, k_{cat} is the turnover number, E_t is the enzyme concentration, A is the substrate concentration, and K_m is the Michaelis constant. For the pH−rate profiles, the effect of pH on k_{cat} and k_{cat}/K_m was determined for each substrate by a fit of the data to eqs 2 and 3 using the computer programs of Cleland (*16*). Equation 2 was used to fit the data when the activity diminished at low pH, whereas eq 3 was used when the activity was lost at high pH. In these equations, y is the value of k_{cat} or k_{cat}/K_m, c is the pH-independent value of y, H is the hydrogen ion concentration, and K_a is the dissociation constant of the ionizable group.

$$v/E_t = k_{cat}A/(K_m + A) \quad (1)$$

$$\log y = \log[c/(1 + H/K_a)] \quad (2)$$

$$\log y = \log[c/(1 + K_a/H)] \quad (3)$$

RESULTS

Kinetic Parameters. The k_{cat}, K_m, and k_{cat}/K_m kinetic constants for the biosynthesis and hydrolysis of dihydroorotate by the zinc-substituted form of DHO are presented in Table 1. Consistent with previously reported data with the DHO from *E. coli*, the maximal rate of formation for the synthesis of dihydroorotate from carbamoyl aspartate is slightly faster than the rate of the hydrolysis reaction (*11*). However, the K_m value for dihydroorotate is ∼10-fold lower than that of carbamoyl aspartate, and thus, k_{cat}/K_m for dihydroorotate is ∼1 order of magnitude higher than it is for carbamoyl aspartate. Although the thio-substituted form

Table 1: Kinetic Parameters for Metal-Substituted Forms of Dihydroorotase[a]

enzyme	substrate	k_{cat} (s^{-1})	K_m (mM)	k_{cat}/K_m (M^{-1} s^{-1})
Zn/Zn-DHO	carbamoyl aspartate	160 ± 8	1.70 ± 0.2	1.0 (0.1) × 10^5
	dihydro-orotate	100 ± 1.6	0.080 ± 0.001	1.2 (0.1) × 10^6
	thiodihydro-orotate	4.4 ± 0.2	0.030 ± 0.001	1.5 (0.3) × 10^5
Co/Co-DHO	carbamoyl aspartate	25 ± 1.4	15 ± 0.2	1.6 (0.2) × 10^3
	dihydro-orotate	15 ± 1.4	0.70 ± 0.03	2.1 (0.2) × 10^4
Cd/Cd-DHO	carbamoyl aspartate	8.2 ± 0.2	4.0 ± 0.9	4.3 (0.1) × 10^3
	dihydro-orotate	1.9 ± 0.3	0.23 ± 0.06	8.3 (0.1) × 10^3
	thiodihydro-orotate	0.42 ± 0.01	0.009 ± 0.001	4.8 (0.9) × 10^4

[a] These data were collected at pH 5.8 with carbamoyl aspartate as the substrate and at pH 8.0 with dihydroorotate or thiodihydroorotate as the substrate.

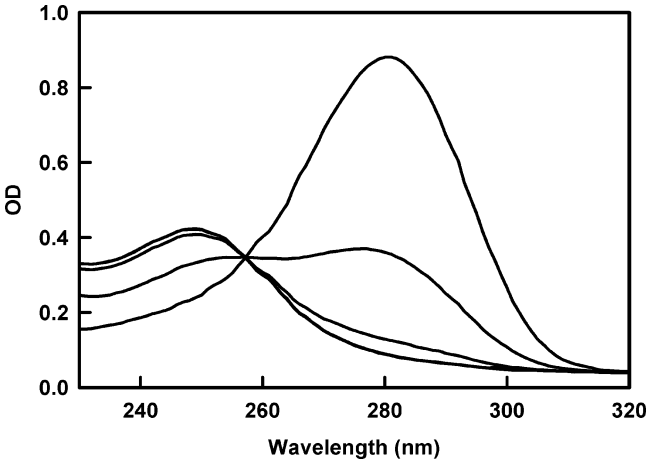

FIGURE 2: Time course for the hydrolysis of TDO at pH 8.0. TDO absorbs with a pH maximum at 280 nm. After the addition of 0.2 μM DHO, spectra were recorded at 2, 4, and 12 min. The absorbance maximum at 280 nm diminishes with time and is replaced by an absorbance maximum at 250 nm that is consistent with the formation of the thio acid analogue of carbamoyl aspartic acid.

of dihydroorotate has been reported to be a potent inhibitor of the eukaryotic DHO from hamster, this compound was found to be a reasonably good substrate for the bacterial enzyme (*8*). Shown in Figure 2 are the time courses for the changes in absorbance after the addition of DHO to a solution of TDO. There is a disappearance of the absorbance at 280 nm that is coupled with the appearance of a new species that absorbs at ~250 nm. This observation is consistent with the formation of the thio acid analogue of carbamoyl aspartate since the absorbance maximum of thioglycine is reported to be 247 nm (*17*). The formation of the hydrolyzed thio acid product was confirmed with mass spectrometry by monitoring the appearance of a new compound with an *m*/*z* of 190.97. This value for the product is 18 mass units greater than that for the parent TDO and is consistent with the addition of water to the thioamide substrate. At pH 8.0, TDO is hydrolyzed at a rate that is 23-fold slower than the rate of dihydroorotate hydrolysis, and the kinetic constants are presented in Table 1. The equilibrium constant for the

Scheme 2

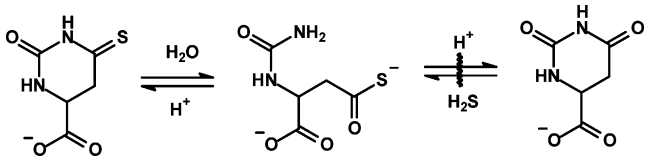

hydrolysis of TDO was determined by measuring the relative magnitude of the absorbances at 280 and 250 nm as a function of pH from 6.0 to 8.0. The data were fit to a modified form of eq 2, and the equilibrium constant was found to be 1.2 × 10^6 M^{-1}. During these experiments, there was no indication for the formation of bisulfide. In addition, incubation of the enzyme with bisulfide (SH^-) and either carbamoyl aspartate or dihydroorotate did not generate a species that absorbs at either 280 or 250 nm at pH 6.0 or 8.0. Therefore, once the thioamide bond of TDO is hydrolyzed, the reverse reaction does not form dihydroorotate with the liberation of bisulfide as illustrated in Scheme 2.

Metal Substitution. The functional role of the two divalent metal ions within the binuclear metal center of DHO was probed via metal substitution experiments. The zinc ions of the native protein were removed by chelation with dipicolinate at pH 5.8 to make the inactive apoenzyme. The binuclear metal center was reconstituted at pH 8.0 by the addition of 2−5 equiv of Zn^{2+}, Co^{2+}, or Cd^{2+}. The metal-substituted variants of DHO were catalytically active according to the following trend: $Zn^{2+} > Co^{2+} > Cd^{2+}$. The values for k_{cat}, K_m, and k_{cat}/K_m of the reconstituted Zn^{2+}, Co^{2+}, and Cd^{2+} enzymes are shown in Table 1. The Cd-substituted DHO was also utilized as a catalyst for the hydrolysis of TDO, and the kinetic constants are presented in Table 1. With Cd-substituted DHO, the K_m for TDO is significantly lower than it is for the hydrolysis of dihydroorotate. In addition, the value of k_{cat}/K_m for the hydrolysis of TDO is 5-fold higher than it is for the hydrolysis of dihydroorotate.

pH−Rate Profiles. Ionizations within the active site of DHO that are critical for the maintenance of catalytic activity were identified by measuring the kinetic constants in both the forward and reverse directions as a function of pH. The pH−rate profiles showing the dependence of the kinetic parameters, k_{cat} and k_{cat}/K_m, were determined for all three substrates, and the plots are presented in Figure 3. The log k_{cat} and log k_{cat}/K_m versus pH profiles (Figure 3A,B) with carbamoyl aspartate as the substrate show that a single group must be *protonated* for optimal activity. The pH−rate profiles for the hydrolysis of either dihydroorotate or TDO indicate that a single group that must be *unprotonated* for activity is critical for catalytic activity (Figure 3C−F). The pH−rate profiles for the hydrolysis and synthesis of dihydroorotate were measured for the Co/Co-substituted enzyme, and the results are also presented in Table 2. For the hydrolysis of dihydroorotate, the kinetic pK_a values observed for the effect of pH on k_{cat} and k_{cat}/K_m are shifted to higher values relative to the pK_a values determined with the Zn/Zn-substituted enzyme.

Solvent Deuterium Isotope Effects. The pH−rate profiles for the Zn-substituted enzyme for the hydrolysis and synthesis of dihydroorotate were measured in the presence of D_2O, and the kinetic pK_a values are presented in Table 2. In general, the kinetic pK_a values are shifted to slightly higher

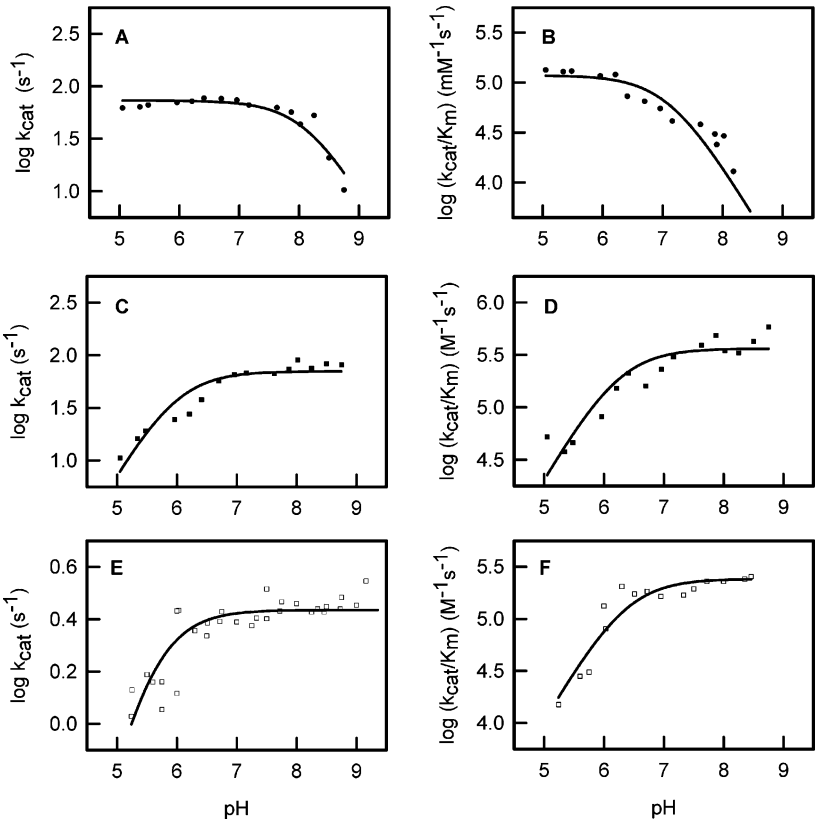

FIGURE 3: pH dependence of the reactions catalyzed by DHO with carbamoyl aspartate (A and B), dihydroorotate (C and D), or thiodihydroorotate (E and F) as the varied substrate.

Table 2: Kinetic pK_a Values from pH−Rate Profiles and Solvent Isotope Effects[a]

substrate	solvent	pK k_{cat}	pK k_{cat}/K_m	solvent isotope effects $^{D}k_{cat}$	solvent isotope effects $^{D}k_{cat}/K_m$
carbamoyl aspartate	H_2O	8.2 ± 0.1	7.1 ± 0.1	1.9 ± 0.2	1.7 ± 0.1
	D_2O	>8.5	7.1 ± 0.2		
	H_2O[b]	7.8 ± 0.2	7.0 ± 0.2		
dihydro-orotate	H_2O	6.0 ± 0.1	6.2 ± 0.2	2.5 ± 0.1	1.1 ± 0.1
	D_2O	5.8 ± 0.1	7.2 ± 0.1		
	H_2O[b]	6.9 ± 0.1	7.6 ± 0.1		
thiodihydro-orotate	H_2O	5.5 ± 0.2	6.4 ± 0.1	2.3 ± 0.1	1.6 ± 0.1
	D_2O	5.9 ± 0.1	6.4 ± 0.3		

[a] Zn-substituted DHO was utilized for these experiments at 30 °C, except as noted. [b] Co-substituted DHO was utilized for these experiments. The pK_a values were obtained by a fit of the data to eq 2 or 3.

values relative to the values obtained for the same parameter measured in H_2O. Similar trends are observed for the hydrolysis of TDO. The pH-dependent equilibrium constant for the interconversion of carbamoyl aspartate and dihydroorotate precluded the accurate measurement of the kinetic constants for formation of dihydroorotate at pH values greater than 8.2 in D_2O. The solvent deuterium isotope effects were measured for all three substrates in the pH-independent region of the pH−rate profiles, and the results are presented in Table 2. A solvent deuterium isotope effect of ~2.1 was obtained on k_{cat} for all three substrates. The largest effect was found on the k_{cat} for the hydrolysis of dihydroorotate, and somewhat smaller effects were obtained for carbamoyl aspartate and TDO. The solvent isotope effects were slightly smaller on k_{cat}/K_m with values ranging from 1.1 to 1.7.

Site-Directed Mutagenesis. The role of specific amino acids in the binding and catalytic interconversion of substrates in DHO was addressed by site-directed mutagenesis. The X-ray structure of DHO shows that the α-carboxylate group of dihydroorotate is coordinated to the active site via multiple electrostatic interactions to Arg-20, Asn-44, and His-254 as illustrated in Figure 4. Mutation of substrate-binding residues Arg-20, Asn-44, and His-254 had a significant effect on the catalytic activity, and the kinetic constants are presented in Table 3. The H254N variant had less than 1% of the activity possessed by the wild-type enzyme. A similar reduction in catalytic activity was obtained with the N44A mutant enzyme. The R20M mutant was inactive, but the R20K variant retained significant activity, with a k_{cat} value of 15 s^{-1}.

It has been postulated that the side chain carboxylate of Asp-250 shuttles the proton from the bridging hydroxide to the leaving group amide of carbamoyl aspartate during the interconversion of the substrate and product (*5*). Five variations of the residue at position 250 of DHO were constructed and characterized using carbamoyl aspartate as the substrate. The conservative replacement in the D250E mutant had the highest activity with a k_{cat} of 12 s^{-1}, relative to a turnover number of 160 s^{-1} for the wild-type enzyme. The catalytic activity of the D250S mutant was diminished by a factor of 4000 in comparison with that of the wild-type enzyme. The turnover numbers for D250A, D250H, and D250N were reduced by more than 4 orders of magnitude relative to that of the wild-type enzyme. The kinetic constants are presented in Table 3. The pH−rate profile for the D250S

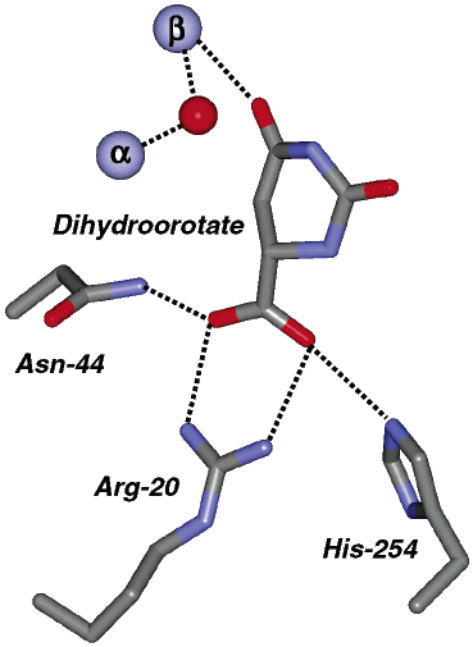

FIGURE 4: Representation of the electrostatic interactions between the α-carboxylate of dihydroorotate and the side chains of Arg-20, Asn-44, and His-254. The coordinates were taken from Thoden et al. (*5*) and obtained from the Protein Data Bank (entry 1J79).

Table 3: Kinetic Parameters for Mutants of Dihydroorotase[a]

	k_{cat} (s^{-1})	K_m (mM)	k_{cat}/K_m (M^{-1} s^{-1})
wild type	160 ± 8	1.7 ± 0.2	1.5 (0.2) × 10^5
D250A	<0.01[b]	nd[b]	nd[b]
D250E	12 ± 1	1.9 ± 0.3	6.3 (0.3) × 10^3
D250H	<0.01[b]	nd[b]	nd[b]
D250N	<0.01[b]	nd[b]	nd[b]
D250S	0.022 ± 0.002	0.51 ± 0.1	4.3 (0.1) × 10^1
R20Q	<0.01[b]	nd[b]	nd[b]
R20K	15 ± 1	0.9 ± 0.1	1.7 (0.1) × 10^4
R20M	<0.01[b]	nd[b]	nd[b]
N44A	<0.01[b]	nd[b]	nd[b]
H254N	<0.01[b]	nd[ba]	nd[b]

[a] The kinetic constants reported here are for the cyclization of carbamoyl aspartate. [b] Not determined because of the detection limit of the assay. These experiments were conducted at a carbamoyl aspartate concentration of 10 mM.

mutant was measured using carbamoyl aspartate as the substrate. The kinetic pK_a for the group that must be protonated for activity was found to be 7.0 ± 0.1.

DISCUSSION

The three-dimensional X-ray structure of DHO has provided a unique view of the active site of this enzyme and the manner in which dihydroorotate and carbamoyl aspartate are associated with the binuclear metal center (*5*). The trapping of the substrate and product within a single protein crystal has enabled a relatively rare glimpse of the molecular interactions of the two reactants in an enzymatic transformation immediately before and after the bond-making and bond-breaking events. This image of the active site has laid the groundwork for the proposed reaction mechanism and subsequent biochemical verification. The reversible hydrolysis of dihydroorotate likely requires three modes of catalysis by DHO: (i) the hydrolytic water molecule must be activated for nucleophilic attack, (ii) the amide bond of the substrate must be made more electrophilic by polarization of the carbonyl−oxygen bond, and (iii) the leaving group nitrogen must be protonated as the carbon−nitrogen bond is cleaved. The catalytic properties of the wild-type enzyme and selected mutants of DHO are consistent with a chemical mechanism that incorporates all three forms of substrate activation.

Activation of Solvent Water. The X-ray structure of DHO in the presence of bound dihydroorotate reveals that there is a single solvent molecule associated with the binuclear metal center. The lone molecule from the solvent is found bridging the two divalent cations as illustrated in Figure 1. The pH−rate profile for the enzymatic hydrolysis of dihydroorotate shows that a single group associated with the protein must be unprotonated for catalytic activity. The loss of catalytic functionality as the pH is lowered is consistent with the protonation of the hydroxide that is proposed to bridge the two divalent cations within the active site of DHO. However, these kinetic studies do not unambiguously address the protonation state of the solvent molecule that bridges the two divalent cations. Nevertheless, in the direction of dihydroorotate hydrolysis, the kinetic pK_a for the Zn-substituted DHO is ~6.1 for k_{cat} and k_{cat}/K_m and is elevated to 6.9 and 7.6 for k_{cat} and k_{cat}/K_m, respectively, for the Co-substituted DHO. Therefore, the specific metal ion associated with the binuclear metal center dictates the pK_a for the loss of catalytic activity at low pH. These results differ from what was found with the hamster enzyme as it was reported that the kinetic pK_a in the direction of dihydroorotate hydrolysis did not change significantly as the divalent cation was substituted with other metal ions (*4*).

The pH−rate profile is different in the direction for the synthesis of dihydroorotate from carbamoyl aspartate. Activity is lost as some group within the active site loses a proton. Microscopic reversibility dictates that this is the same group that must be unprotonated for catalytic activity during the hydrolysis reaction. Optimization of the biosynthetic reaction would require the protonation of the bridging hydroxide followed by dissociation of the resulting water molecule upon the binding of carbamoyl aspartate. This conclusion is supported by the X-ray structure of DHO in the presence of carbamoyl aspartate (*5*). In this enzyme−substrate complex, the carboxylate group of carbamoyl aspartate was found bridging the two divalent cations. There was no other water molecule coordinated to either metal ion. The kinetic pK_a values measured for k_{cat}/K_m with the Zn-substituted DHO in the two directions are not the same, and thus, the apparent ionization constant for the bridging water or hydroxide must be influenced by the stickiness of one or both of the substrates (*18*). From the relative values of K_m and k_{cat}/K_m for carbamoyl aspartate and dihydroorotate, it is likely that dihydroorotate is stickier than carbamoyl aspartate.

Polarization of the Substrate. The activation of dihydroorotate as an electrophile is expected to be enhanced through polarization of the carbonyl group of the substrate. Complexation of dihydroorotate in the active site of DHO via a direct interaction of the carbonyl oxygen with the metal center would diminish the electron density at the carbon center and facilitate nucleophilic attack by the bridging hydroxide. This type of substrate activation is observed in the crystal structure of dihydroorotate bound to the Zn-substituted DHO. In this structure, the carbonyl oxygen is

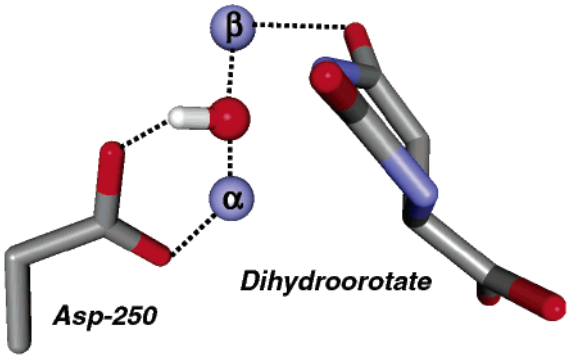

FIGURE 5: Relative orientation of Asp-250 and the hydroxide that bridges the two divalent cations within the active site of dihydroorotase (PDB entry 1J79). The proposed orientation of the hydrogen is shown for the purposes of discussion only.

2.9 Å from the β-metal ion. The direct interaction of the metal center with the carbonyl oxygen of the amide bond to be cleaved is also supported by the kinetic properties of DHO upon substitution of sulfur for oxygen in the substrate using TDO. The more easily polarized sulfur is expected to form a complex better with the softer cadmium than with the harder zinc. In the cadmium-substituted enzyme, the k_{cat}/K_m for TDO is 5-fold higher than with the Zn-substituted DHO, whereas with the Zn-substituted DHO, the k_{cat}/K_m for dihydroorotate is 1 order of magnitude higher than it is for TDO.

Protonation of the Leaving Group. During the hydrolysis of dihydroorotate, the amide nitrogen must be protonated. Conversely, during the synthesis of dihydroorotate, a proton must be abstracted from the attacking amide nitrogen. In the X-ray structure of DHO, there are no acid−base groups that can facilitate this proton transfer except for Asp-250 from strand 8 that is also ligated to the α-metal ion. This residue has been proposed as the group that shuttles the proton from the bridging hydroxide to and from the substrate and product during the course of the reaction (*5*). Shown in Figure 5 is a representation of the active site of DHO showing the relative positions of dihydroorotate, Asp-250, the two divalent cations, and the bridging hydroxide. In this structure, the hydroxide that bridges the two divalent cations is poised to attack the carbonyl carbon of the bound dihydroorotate. If one positions the bound hydrogen and the remaining lone pair attached to the oxygen in a tetrahedral arrangement with regard to the ligation to the two divalent cations, then the hydrogen is logically placed in a hydrogen bonding interaction with the carboxylate from Asp-250 and the lone pair is oriented directly toward the carbonyl carbon. The essential nature of Asp-250 for proton transfer reactions was addressed via site-directed mutagenesis. This residue was substituted with alanine, glutamate, histidine, asparagine, and serine. Of these residues, the substitution with glutamate was the only perturbation that was tolerated at this position with any significant catalytic activity. The D250E mutant retained 7.5% of the value of k_{cat} compared to the wild-type DHO from *E. coli*. In the hamster enzyme, mutation of the homologous aspartate residue to glutamate resulted in an enzyme that had a k_{cat} that was less than 10% of that of the wild-type enzyme and experienced a 14-fold increase in K_m (*19*). The aspartate from strand 8 that resides in the active site of the related enzyme phosphotriesterase has also been demonstrated to be involved in proton transfer reactions with

Scheme 3

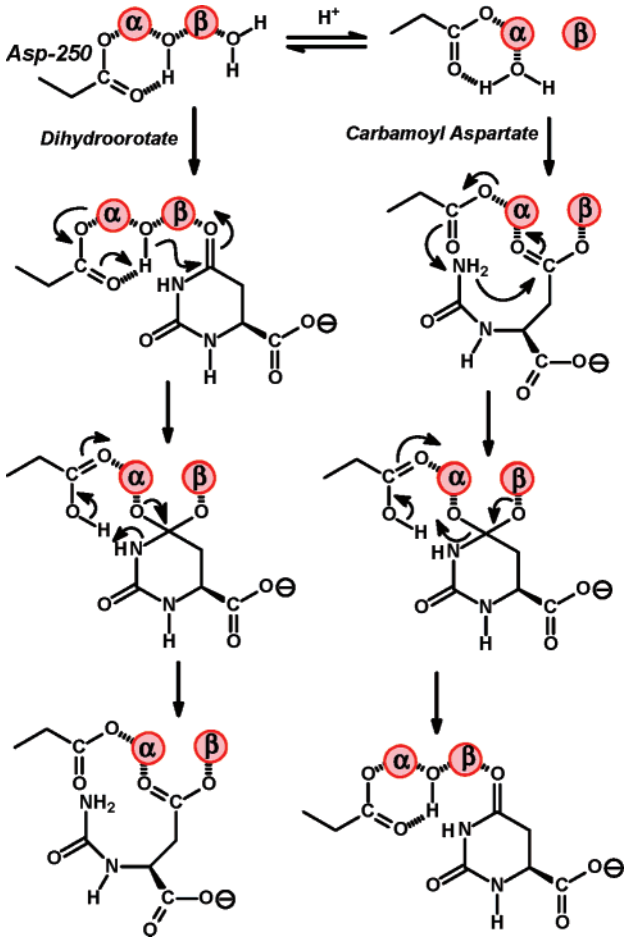

the bridging hydroxide (*20*). The solvent isotope effects measured for the formation and hydrolysis of dihydroorotate are modest. At this point, it is not possible to determine if this reflects the effect of deuterium on the proton transfer during substrate attack or whether this is a reflection of the recharging of the binuclear metal center from water after each turnover of the substrate.

Substrate Binding Interactions. The exocyclic α-carboxylate group of dihydroorotate is bound to the protein via electrostatic interactions with the side chains of Arg-20, Asn-44, and His-254. Mutation of any of these residues abolishes the ability to cyclize carbamoyl aspartate to dihydroorotate with the single exception of the replacement of Arg-20 with lysine. Loss of enzymatic activity was also seen when the homologous residues were mutated in the hamster enzyme (*19*, *21*). It is clear from these results that the active site of DHO has a rather stringent requirement for substrate binding. In this regard, we have attempted to hydrolyze dihydrouracil with the wild-type DHO without success.

Mechanism of Action. The characterization of the catalytic properties of the wild-type and mutated forms of DHO coupled with the high-resolution X-ray crystal structure has provided sufficient insights for the assembly of a self-consistent chemical mechanism for the interconversion of the substrate and products within the active site of this enzyme. The reaction mechanism is presented in Scheme 3. For the hydrolysis of dihydroorotate, it is proposed that the active form of the enzyme is one in which a hydroxide is bridging the two divalent cations within the enzyme active

site. Dihydroorotate binds to the binuclear metal center where the carbonyl oxygen is ligated to the β-metal which polarizes the carbonyl group. This orientation is supported by the X-ray structure of the bound dihydroorotate and the relative kinetic properties of the thio-substituted dihydroorotate (*5*). Nucleophilic attack by the bridging hydroxide is facilitated by the transfer of the proton from the hydroxide to the carboxylate coordinated to the α-metal ion. A tetrahedral adduct is formed that bridges the two divalent cations. Collapse of the tetrahedral adduct occurs with protonation of the amide nitrogen and cleavage of the carbon−nitrogen bond. The resulting carbamoyl aspartate is coordinated to the binuclear metal center via the newly formed carboxylate group. This structure is supported by the X-ray structure of the bound carbamoyl aspartate (*5*). The product is released, and the binuclear metal center is recharged with hydroxide via a process that has not been addressed by the experiments presented in this paper. In the reverse direction, the carbamoyl aspartate binds to the protonated form of the enzyme with the release of a bound water molecule. In this direction, the reaction is initiated by the abstraction of a proton from the amide nitrogen by the carboxylate of Asp-250 concomitant with nucleophilic attack of the amide nitrogen on the carboxylate of carbamoyl aspartate that is bridging the binuclear metal center.

REFERENCES

1. Fields, C., Brichta, D., Shepherdson, M., Farinha, M., and O'Donovan, G. (1999) Phylogenetic Analysis and Classification of Dihydroorotases: A Complex History for a Complex Enzyme, *Pathways to Pyrimidines: An International Newsletter 7*, 49−63.
2. Jones, M. E. (1980) Pyrimidine nucleotide biosynthesis in animals: Genes, enzymes, and regulation of UMP biosynthesis, *Annu. Rev. Biochem. 49*, 253−279.
3. Musmanno, L. A., Jamison, R. S., Barnett, R. S., Buford, E., and Davidson, J. N. (1992) Complete hamster CAD protein and the carbamoyl phosphate synthetase domain of CAD complement mammalian cell mutants defective in *de novo* pyrimidine biosynthesis, *Somatic Cell Mol. Genet. 18*, 309−318.
4. Huang, D. T., Thomas, M. A., and Christopherson, R. I. (1999) Divalent metal derivatives of the hamster dihydroorotase domain, *Biochemistry 38*, 9964−9970.
5. Thoden, J. B., Phillips, G. N., Jr., Neal, T. M., Raushel, F. M., and Holden, H. M. (2001) Molecular structure of dihydroorotase: A paradigm for catalysis through the use of a binuclear metal center, *Biochemistry 40*, 6989−6997.
6. Holm, L., and Sander, C. (1997) An evolutionary treasure: Unification of a broad set of amidohydrolases related to urease, *Proteins: Struct., Funct., Genet. 28*, 72−82.
7. Christopherson, R. I., and Jones, M. E. (1980) The effects of pH and inhibitors upon the catalytic activity of the dihydroorotase of multienzymatic protein pyr1−3 from mouse Ehrlich ascites carcinoma, *J. Biol. Chem. 255*, 3358−3370.
8. Christopherson, R. I., Schmalzl, K. J., Szabados, E., Goodridge, R. J., Harsanyi, M. C., Sant, M. E., Algar, E. M., Anderson, J. E., Armstrong, A., Sharma, S. C., Bubb, W. A., and Llyons, S. D. (1989) Mercaptan and dicarboxylate inhibitors of hamster dihydroorotase, *Biochemistry 28*, 463−470.
9. Washabaugh, M. W., and Collins, K. D. (1986) Dihydroorotase from *Escherichia coli*. Sulfhydryl group-metal ion interactions, *J. Biol. Chem. 261*, 5920−5929.
10. Daniel, R., Caminade, E., Martel, A., Le Goffic, F., Canosa, D., Carrascal, M., and Abian, J. (1997) Mass spectrometric determination of the cleavage sites in *Escherichia coli* dihydroorotase induced by a cysteine-specific reagent, *J. Biol. Chem. 272*, 26934−26939.
11. Washabaugh, M. W., and Collins, K. D. (1984) Dihydroorotase from *Escherichia coli*. Purification and characterization, *J. Biol. Chem. 259*, 3293−3298.
12. Ho, S. N., Hunt, H. D., Horton, R. M., Pullen, J. K., and Pease, L. R. (1989) Site-directed mutagenesis by overlap extension using the polymerase chain reaction, *Gene 77*, 51−59.
13. Sander, E. G., Wright, L. D., and McCormick, D. B. (1965) Evidence for function of a metal ion in the activity of dihydroorotase from *Zymobacterium oroticum*, *J. Biol. Chem. 240*, 3628−3630.
14. Taylor, W. H., Taylor, M. L., Balch, W. E., and Gilchrist, P. S. (1976) Purification and properties of dihydroorotase, a zinc-containing metalloenzyme in *Clostridium oroticum*, *J. Bacteriol. 127*, 863−873.
15. Schowen, K. B., and Schowen, R. L. (1982) Solvent isotope effects of enzyme systems, *Methods Enzymol. 87*, 551−606.
16. Cleland, W. W. (1979) Statistical analysis of enzyme kinetic data, *Methods Enzymol. 63*, 103−138.
17. Weast, R. C., and Astle, M. J. (1985) HODOC No: 21011, *CRC Handbook of Data on Organic Compounds*, CRC Press, Boca Raton, FL.
18. Cleland, W. W. (1982) The Use of pH Studies to Determine Chemical Mechanisms of Enzyme-Catalyzed Reactions, *Methods Enzymol. 87*, 390−405.
19. Williams, N. K., Manthey, M. K., Hambley, T. W., O'Donoghue, S. I., Keegan, M., Chapman, B. E., and Christopherson, R. I. (1995) Catalysis by hamster dihydroorotase: Zinc binding, site-directed mutagenesis, and interaction with inhibitors, *Biochemistry 34*, 11344−11352.
20. Aubert, S. A., Li, Y., and Raushel, F. M. (2004) Mechanism for the hydrolysis of organophosphates by the bacterial phosphotriesterase, *Biochemistry 43*, 5707−5715.
21. Zimmermann, B. H., Kemling, N. M., and Evans, D. R. (1995) Function of conserved histidine residues in mammalian dihydroorotase, *Biochemistry 34*, 7038−7046.

BI048308G